Original Article | Balkan Med J

Fucoxanthin Attenuates Bisphenol A-Induced Testicular Injury via NF-κB-Mediated Pyroptosis Inhibition

Ke Xu#, Xiangyu Ren#, Hongjie Cao, Tiantian Lyu, Zuisu Yang, Fangfang Huang

Zhejiang Ocean University School of Food and Pharmacy, Zhejiang Provincial Technology Research Center of Marine Biomedical Products, Zhoushan, China

#These authors contributed equally to this work.

Background: Bisphenol A (BPA), a widely used industrial chemical, is a well-known endocrine disruptor linked to testicular damage and impaired male reproductive function. Fucoxanthin (Fx), a marine carotenoid with potent antioxidant properties, has not been extensively studied for its potential to mitigate BPA-induced testicular injury.

Aims: This study evaluated the protective effects of Fx against BPA-induced testicular injury and explored the underlying signaling mechanisms.

Study Design: Experimental study.

Methods: A mouse model of BPA-induced testicular injury was established. Transcriptomic analysis was performed to identify significantly altered genes. The therapeutic potential of Fx was assessed using combined molecular and histological approaches. Complementary *in vitro* experiments with TM3 Leydig cells were conducted to support the *in vivo* findings.

Results: Fx administration markedly attenuated BPA-induced disruptions in serum sex hormones, testicular histopathology, and proinflammatory cytokine levels. Ribonucleic acid sequencing revealed that Fx's protective effects are associated with modulation of the nuclear factor kappa B (NF-κB), nucleotide-binding oligomerization domain-like, and Toll-like receptor signaling pathways. Validation experiments indicated that Fx inhibits nucleotide-binding oligomerization domain-like receptor family pyrin domain-containing 3 (NLRP3) inflammasome activation and suppresses pyroptosis, accompanied by downregulation of key genes and proteins in the lipopolysaccharide/NLRP3 signaling cascade. *In vitro* analyses confirmed that Fx reduces oxidative stress and inflammation by inhibiting NF-κB activation and pyroptosis.

Conclusion: These findings suggest that Fx may serve as a promising dietary supplement or nutraceutical agent to mitigate the adverse reproductive effects of environmental endocrine disruptors, with potential benefits for male reproductive health.

INTRODUCTION

Bisphenol A (BPA), a key monomer in plastics and resins, is a widespread environmental contaminant and a well-characterized endocrine-disrupting chemical.[1-3] Humans are routinely exposed to BPA, and both epidemiological and experimental studies have consistently linked it to male reproductive impairments, including hormonal imbalances, developmental toxicity, and testicular dysfunction.[4,5] The underlying mechanisms are complex, involving oxidative stress, inflammatory responses, mitochondrial dysfunction, and blood–testis barrier disruption, which collectively compromise testicular homeostasis.[6,7]

Sustained oxidative stress activates nuclear factor kappa B (NF-κB), which regulates the expression of numerous proinflammatory mediators, including components of the nucleotide-binding oligomerization domain-like receptor family pyrin domain-containing 3 (NLRP3) inflammasome. Activation of caspase-1 by the assembled NLRP3 inflammasome triggers gasdermin D (GSDMD) cleavage, culminating in pyroptosis—a lytic, proinflammatory form of programmed cell death.[8] Recent studies indicate that BPA exposure can induce pyroptosis in multiple cell types, highlighting this pathway as a critical, yet underexplored, mechanism of BPA-induced testicular damage.[9-12] Consequently, targeting pyroptosis presents a promising therapeutic strategy.

Fucoxanthin (Fx), a marine carotenoid, exhibits potent anti-inflammatory, antioxidant, and antidiabetic properties.[13-15] These attributes have fueled interest in Fx as a candidate for nutraceutical and pharmaceutical development.[16,17] Although Fx has demonstrated

Corresponding authors: Zuisu Yang and Fangfang Huang, Zhejiang Ocean University School of Food and Pharmacy, Zhejiang Provincial Technology Research Center of Marine Biomedical Products, Zhoushan, China

e-mail: yzs@zjou.edu.cn, gracegang@126.com

Received: December 3, 2025 **Accepted:** February 19, 2026 **Available Online Date:** • **DOI:** 10.4274/balkanmedj.galenos.2026.2025-11-268

Available at www.balkanmedicaljournal.org

ORCID iDs of the authors: K.X. 0009-0003-5873-2298; X.R. 0000-0001-9434-4151; H.C. 0000-0001-9845-1413; T.L. 0009-0004-0745-378X; Z.Y. 0009-0008-0667-6104; F.H. 0009-0004-3490-7986.

Cite this article as: Xu K, Ren X, Cao H, et al. Fucoxanthin Attenuates Bisphenol A-Induced Testicular Injury via NF-κB-Mediated Pyroptosis Inhibition.. Balkan Med J.;

protective effects against testicular injury induced by streptozotocin–nicotinamide and cisplatin, its potential efficacy against BPA-induced reproductive toxicity, and its capacity to modulate pyroptosis in this context, remain unexplored.[18,19]

To address this gap in environmental reproductive health, we investigated the protective effects of Fx against BPA-induced testicular injury. We hypothesized that Fx confers protection not only through antioxidant activity but also by suppressing the BPA-activated NF-κB/NLRP3 axis, thereby inhibiting downstream pyroptotic cell death. Using integrated *in vivo* (mouse) and *in vitro* (TM3 Leydig cell) models, this study emphasizes the potential of Fx as a dietary intervention to mitigate BPA-associated impairment of male reproductive function.

MATERIALS AND METHODS

Reagents and antibodies

Fx (≥ 95% purity) was supplied by Shandong Jiejing Group Co., Ltd. (Shandong, China). BPA (≥ 99% purity; B108652-25g) was obtained from Shanghai Aladdin Biochemical Technology Co., Ltd. (Shanghai, China). C34 was purchased from Bide Pharmatech Co., Ltd. (Shanghai, China). The TM3 Leydig cell line (CL0234), TM3 Cell Complete Medium (CM-0234), and DMEM/F12 (PM150312) were provided by Procell Life Science & Technology (Wuhan, China).

The following kits from TransGen Biotech (Beijing, China) were used: TransZol Up Plus ribonucleic acid (RNA) Kit (ER501-01), All-in-One First-Strand complementary DNA (cDNA) Synthesis SuperMix (AT341-01), and PerfectStart Green qPCR SuperMix (AQ601-01). Assay kits for total superoxide dismutase (T-SOD, A001-1), malondialdehyde (MDA, A003-1), glutathione peroxidase (GSH-PX, A005-1), and catalase (CAT, A007-1) were purchased from Nanjing Jiancheng Bioengineering Institute (Nanjing, China). Enzyme-linked immunosorbent assay (ELISA) kits for tumor necrosis factor-α (TNF-α) (KE10002) and interleukin-1β (IL-1β) (KE10003) were obtained from Proteintech Group, Inc. (Wuhan, China), and IL-18 (E-EL-M0730) from Elabscience Biotechnology Co., Ltd. (Wuhan, China). Hormone and cytokine assay kits for testosterone (TE, SP14088), luteinizing hormone (LH, SP14102), interferon-α (IFN-α) (SP13692), and interferon-β (IFN-β) (SP13645) were purchased from Wuhan Saipei Biotechnology Co., Ltd. (Wuhan, China).

DAPI (C0060) and testicular tissue fixative (FSA fixative, G2362) were obtained from Beijing Solarbio Science & Technology Co., Ltd. (Beijing, China). Cell Counting Kit-8 (CCK-8, C0038) was purchased from Beyotime Biotech Inc. (Shanghai, China), and the Cell Cycle Detection Kit (KGA511-KGA512) from Jiangsu KeyGEN BioTECH Corp., Ltd. (Jiangsu, China).

Animal and grouping

Sixty 3-week-old male C57BL/6J mice were obtained from Qizhen Experimental Animal Technology Co., Ltd. [license number SCXK (Zhe) 2022-0005]. In accordance with the Guiding Principles in the Care and Use of Animals of China, mice were housed in a pathogen-free facility [license number SYXK (Zhe) 2019-0031] under controlled temperature (23 ± 2 °C) and humidity (40–70%) on a 12-h light/dark cycle. The experimental protocol was approved by the Ethics Committee of Zhejiang Ocean University (approval number: 2023113, date: 20.12.2023). After a one-week acclimation period, the mice were randomly assigned to the following groups (n = 12 per group): control (Con), BPA (5 mg/kg), C34 + BPA (1 mg/kg C34 and 5 mg/kg BPA), low-dose Fx + BPA (20 mg/kg Fx and 5 mg/kg BPA), and high-dose Fx + BPA (40 mg/kg Fx and 5 mg/kg BPA). All compounds were administered orally in equivalent volumes, with the control group receiving deionized water. Following the 8-week treatment period, mice were euthanized, and testicular tissues and blood samples (for serum preparation) were collected for subsequent analyses.

The main cohort sample size (n = 12 per group) was selected in accordance with the 3R principle and standard practice in rodent toxicology studies, which typically employ 8–12 animals for robust phenotypic assessment.[20,21] A subsequent power analysis confirmed that this design provided 80% power (α = 0.05) to detect large effect sizes (Cohen's f ≈ 0.40) for primary outcomes. To maximize data yield while preserving tissue integrity for distinct assays, a stratified sampling approach was applied. Following tissue allocation for primary phenotyping, a subset of samples (n = 3–6 per group) was randomly selected for molecular analyses. A tolerable daily intake (TDI) of 0.2 ng/kg body weight/day has been established for BPA by the European Food Safety Authority. Although the selected BPA dose exceeded the TDI, it is consistent with previous studies for reliably inducing testicular injury and investigating its molecular mechanisms.[22,23] The Fx doses (20 and 40 mg/kg) were chosen based on prior preclinical studies demonstrating both efficacy and safety in organ protection.[24] A 1 mg/kg dose of the TLR4 inhibitor C34 served as a positive control, in line with evidence that BPA-induced injury involves TLR4/NF-κB activation.[25,26]

Biochemical parameters in serum and testis

Following the protocols provided with the commercial kits, oxidative stress markers—including MDA, CAT, T-SOD, and GSH-Px—were measured in testicular homogenates. Additionally, concentrations of TNF-α, IL-1β, IFN-α, and IFN-β in testicular tissues, as well as TE and LH in serum, were determined.

H&E staining, immunohistochemistry, and immunofluorescence

Testicular tissues were fixed in FSA fixative for 48 hours, dehydrated through a graded ethanol series, cleared with xylene, and subsequently embedded in paraffin. The paraffin blocks were then sectioned at 4 μm.

For histological analysis, tissue sections were processed through a graded ethanol series and rehydrated in distilled water. Nuclei were stained with hematoxylin, and cytoplasm was stained with eosin.

For immunohistochemistry, the following primary antibodies were used: p65 (1:100), Caspase-1 (1:100), Caspase-11 (1:100), NLRP3 (1:100), and occludin (1:500). Sections were imaged under an Olympus microscope (Japan), and the total area of positive staining was semi-quantified using ImageJ software (National Institutes of Health, USA).

For immunofluorescence, primary antibodies included MARS2 (1:100) and lipopolysaccharide (LPS) (1:100). Coverslips were photographed under a fluorescence microscope (Carl Zeiss AG, Germany), and semi-quantitative analysis of average fluorescence intensity was performed using ImageJ Fiji (National Institutes of Health, USA).

To ensure objective documentation and analysis, all procedures involving subjective assessment were performed in a blinded manner. Both image acquisition and subsequent quantitative analyses for histopathological, immunohistochemical, and immunofluorescence evaluations of tissue sections and cultured cells were conducted by researchers blinded to experimental group assignments.

Sequencing and analysis of testicular transcriptomics

Transcriptomic sequencing of testicular tissues was performed by Majorbio Technology Co., Ltd. (Shanghai, China). Total RNA was extracted from all experimental groups with three biological replicates per group (n = 3). The RNA integrity number of all samples exceeded 8.0, confirming high-quality input material. After sequencing, raw reads underwent quality control and were aligned to the reference genome. Differentially expressed genes (DEGs) were identified using the DESeq2 R package. *p* values were adjusted using the Benjamini-Hochberg method to control the false discovery rate and reduce false positives arising from multiple comparisons. DEGs were defined as those with $|\log_2 \text{FoldChange}| \geq 1$ and an adjusted *p* value (q value) < 0.05. Functional enrichment analyses of DEGs were performed against the Kyoto Encyclopedia of Genes and Genomes (KEGG) and Gene Ontology databases. Raw sequencing data have been deposited in the NCBI Sequence Read Archive under accession number PRJNA1420001.

Tissue qRT-PCR and western blotting

Total RNA was extracted from testicular tissue using a commercial kit and reverse-transcribed to cDNA. All primers (Table 1) were synthesized by Suzhou ICP Bio-technology Co., Ltd. qPCR assays were conducted on the FQD-48A fluorescence quantitative PCR instrument (Hangzhou Bioer Technology) using the primers and PerfectStart® Green qPCR SuperMix. Gene expression levels were quantified using the $2^{-\Delta\Delta CT}$ method.

Western blot analysis was performed as previously described.[27] Primary antibodies included androgen receptor (AR), MARS2, p53, p-p65, Caspase-1, Caspase-1 p20, Caspase-11, and N-GSDMD (1:1000); STAT1 and p-IκBα (1:2000); TLR4, IκBα, and GSDMD (1:5000); Caspase-11 p20 (1:500); β-actin (1:10,000); and GAPDH (1:100,000).

TABLE 1. Antibodies Information.

Antibodies (catalog number)	Vendor (country)
Occludin (66378-1-Ig)	Proteintech Group, Inc. (Wuhan, China)
p53 (21891-1-AP)	Proteintech Group, Inc. (Wuhan, China)
STAT1 (10144-2-AP)	Proteintech Group, Inc. (Wuhan, China)
NLRP3 (68102-1-Ig)	Proteintech Group, Inc. (Wuhan, China)
TLR4 (66350-1-Ig)	Proteintech Group, Inc. (Wuhan, China)
IκBα (10268-1-AP)	Proteintech Group, Inc. (Wuhan, China)
p-IκBα (82349-1-RR)	Proteintech Group, Inc. (Wuhan, China)
Caspase-1 (31020-1-AP)	Proteintech Group, Inc. (Wuhan, China)
GAPDH (60004-1-Ig)	Proteintech Group, Inc. (Wuhan, China)
β-actin (20536-1-AP)	Proteintech Group, Inc. (Wuhan, China)
p65 (AF5006)	Affinity Biosciences Group, Ltd. (Jiangsu, China)
Caspase-1 p20 (AF4005)	Affinity Biosciences Group, Ltd. (Jiangsu, China)
N-GSDMD (DF13758)	Affinity Biosciences Group, Ltd. (Jiangsu, China)
p-p65 (AF5881)	Beyotime Biotech Inc. (Shanghai, China)
Androgen receptor (AF6198)	Beyotime Biotech Inc. (Shanghai, China)
MARS2 (abs113265)	Absin Bioscience Inc. (Shanghai, China)
Caspase-11 (NB120-10454)	Novus Biologicals (Littleton, USA)
Caspase-11 p20 (sc-374615)	Santa Cruz Biotechnology (Santa Cruz, USA)
LPS (HM6011)	Hycult Biotech (Uden, The Netherlands)
GSDMD (ab219800)	Abcam (Cambridge, UK)

NLRP3, nucleotide-binding oligomerization domain-like receptor family pyrin domain-containing 3; p-IκBα/IκBα, phospho-IκBα to total IκBα; GSDMD, gasdermin D; LPS, LPS, lipopolysaccharide.

Cell culture and grouping

TM3 cells were maintained in complete medium at 37 °C in a 5% CO_2 incubator. After seeding in 96-well plates, cells were treated for 24 hours with indicated doses of BPA (0.01–100 μM), Fx (1–100 μM), or C34 (5 or 10 μM). All treatments were delivered in DMEM/F12 medium containing 0.1% (v/v) dimethyl sulfoxide (DMSO), which served as the negative control. Based on CCK-8 assay results, final concentrations of 50 μM BPA, 5 μM Fx, and 10 μM C34 were selected for subsequent experiments. Each condition was tested in at least three independent experiments.

Detection of IL-18 and IL-1β in cell supernatant by ELISA

Following treatment (Section 2.7), culture medium was collected and centrifuged at 4 °C to obtain a cell-free supernatant. Levels of IL-18 and IL-1β in the supernatant were measured using commercially available ELISA kits according to the manufacturer's protocols.

Immunofluorescence in cultured cells

TM3 cells were seeded in 6-well plates and incubated for 24 hours. For the Fx and C34 groups, cells were pretreated with DMEM/F12 containing 5 μM Fx or 10 μM C34, respectively, for 6 hours, whereas other groups received DMEM/F12. After pretreatment, the Con group received DMEM/F12, while the BPA, Fx, and C34 groups were treated with DMEM/F12 containing 50 μM BPA for 24 hours. Cells were incubated overnight with an anti-p65 antibody (1:100). Fluorescence imaging was performed using a fluorescence microscope (Carl Zeiss AG, Germany).

Cellular qRT-PCR and western blotting

After 24-hour BPA treatment (Section 2.8), cells were digested with 0.25% (w/v) trypsin until partially detached. The reaction was terminated by adding 100 μL of complete TM3 cell medium. Cells were then resuspended and centrifuged to collect the pellet, and total RNA was isolated as described in Section 2.6 for cDNA synthesis.

For Western blotting, cells were washed three times with PBS (5 minutes per wash) following the 24-hour BPA treatment. Cell lysis was performed on ice for 30 minutes using radioimmunoprecipitation assay lysis buffer supplemented with 1% (v/v) phenylmethylsulfonyl fluoride. Lysates were clarified by centrifugation, and Western blot analysis was carried out as outlined in Section 2.6.

Statistical analysis

Due to modest and variable sample sizes across experiments (n = 3–6 per group), all statistical comparisons were performed using non-parametric tests to ensure robustness and avoid assumptions regarding data distribution. The Kruskal–Wallis test was applied for comparisons across multiple groups, followed by Dunn's post-hoc test for pairwise comparisons when appropriate. Data are presented as box-and-whisker plots showing the median, interquartile range, and full range, with individual data points overlaid. Statistical analyses are considered preliminary and exploratory, primarily aimed at identifying consistent trends and generating hypotheses for future validation in larger cohorts. All analyses were performed using GraphPad Prism (version 8.3.0), and p values < 0.05 were considered statistically significant.

RESULTS

BPA exposure induces testicular injury in mice

The established physiological reference ranges for serum hormones in adult male C57BL/6 mice are 0.2–1.5 ng/mL for LH and 3.5–20.8 nmol/L for TE.[28,29] Compared with these reference values and the control group, BPA exposure induced marked testicular injury, as evidenced by a significant reduction in testicular weight and suppression of both TE and LH levels below the physiological range (Figure 1a-c). Treatment with either C34 or Fx effectively alleviated these detrimental effects. Notably, both interventions restored serum TE levels to within the normal reference range (Figure 1b). Histopathological examination using hematoxylin and eosin staining revealed that BPA exposure resulted in thinning of the seminiferous epithelium, disruption of seminiferous tubular architecture, and a reduction in Leydig cell numbers (Figure 1d). Immunohistochemical analysis further demonstrated impaired tight junction integrity between Sertoli cells (Figure 1e). In contrast, administration of C34 or Fx markedly attenuated these BPA-induced histopathological alterations, restoring tissue architecture and cellular organization.

Oxidative stress and inflammatory biomarkers in testicular tissues

To further evaluate the protective effects of Fx against BPA-induced testicular injury, oxidative stress and inflammatory biomarkers were assessed. BPA exposure significantly disrupted testicular

TABLE 2. Primer Information Table.

NCBI ID	Forward primer (5'–3')	Reverse primer (5'–3')
Tlr4/21898	GCCTTTCAGGGAATTAAGCTCC	GATCAACCGATGGACGTGTAAA
Nfkb1/18033	ATGGCAGACGATGATCCCTAC	CGGAATCGAAATCCCCTCTGTT
Nfkb2/18034	GCGGTGGAGACGAAGTTTATT	TCATCCTCATAGAACCGAACCT
Rela/19697	ACTGCCGGGATGGCTACTAT	TCTGGATTCGCTGGCTAATGG
Relb/19698	CACCGGGTACACCCACATAG	ATGCCCAGGTTGTTAAAGCTG
Nlrp3/216799	ATTACCCGCCCGAGAAAGG	CATGAGTGTGGCTAGATCCAAG
Casp1/12362	ACAAGGCACGGGACCTATG	TCCCAGTCAGTCCTGGAAATG
Gsdmd/69146	TTCCAGTGCCTCCATGAATGT	GCTGTGGACCTCAGTGATCT

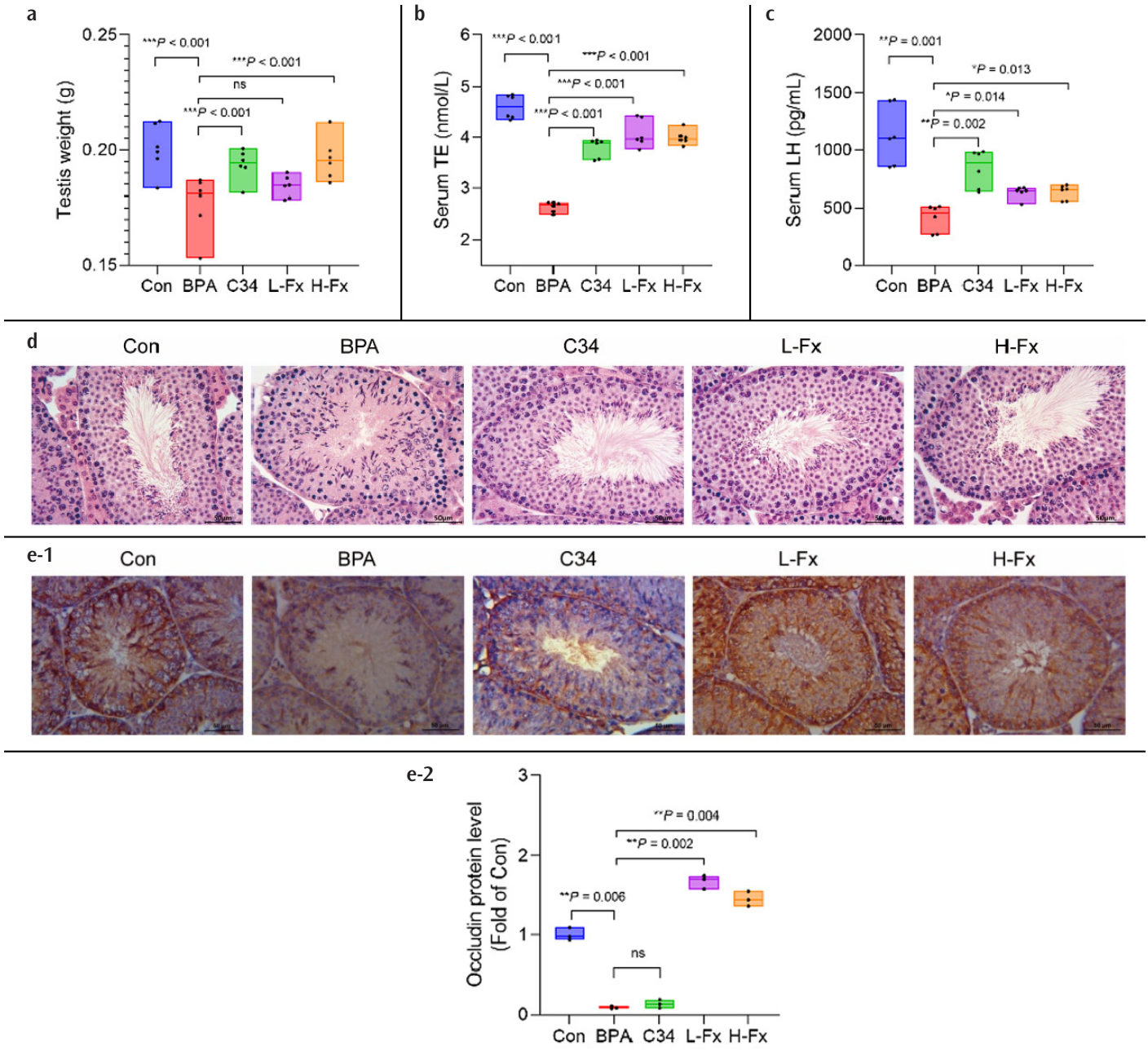

FIG. 1. The effect of Fx on BPA-induced testicular damage in mice. (a) The testis weight of mice; (b, c) the levels of serum LH and TE; (d) histopathological analysis of mouse testis (400 ×); (e) immunohistochemistry images showcasing occludin protein expression in each group (400 ×) and quantified results of occludin protein in the testis. Data are presented as box-and-whisker plots (median, IQR, range) with individual points (n = 6), except for Figure 1e, where n = 3. Groups were compared using the Kruskal–Wallis test followed by Dunn's post-hoc test. *$p < 0.05$, **$p < 0.01$, ***$p < 0.001$. BPA, bisphenol A; Fx, fucoxanthin; TE, testosterone; LH, luteinizing hormone, IQR, interquartile range.

redox homeostasis, as indicated by elevated levels of MDA, a lipid peroxidation marker, and concomitant reductions in the activities of antioxidant enzymes, including CAT, T-SOD, and GSH-Px (Figure 2a-d). Both C34 and Fx treatments mitigated this oxidative imbalance. Specifically, they normalized MDA levels and restored CAT and T-SOD activities, whereas only C34 exhibited a trend toward recovery of GSH-Px activity (Figure 2a-d). BPA exposure also elicited a pronounced inflammatory response, characterized by significantly elevated levels of TNF-α, IL-1β, IFN-α, and IFN-β (Figure 2e-h). Treatment with C34 or Fx significantly suppressed this inflammatory response, reducing the concentrations of all four cytokines (Figure 2e-h).

Testicular transcriptome analysis

Volcano plot analysis was performed to identify DEGs among the experimental groups (Figure 3a). BPA exposure significantly downregulated MARS2 expression, whereas treatment with Fx or the positive control (C34) reversed this effect. Functional enrichment analysis revealed that the identified DEGs were predominantly associated with reproductive developmental processes and, more importantly, with immune and inflammatory signaling pathways, including NF-κB, nucleotide-binding oligomerization domain-like receptor, and Toll-like receptor pathways (Figure 3b, c). Given the established roles of these pathways in mediating immune and inflammatory responses, their modulation may represent a key mechanism by which Fx alleviates BPA-induced testicular injury.

Fx attenuates BPA-induced oxidative stress–mediated testicular injury

In this initial exploratory phase, we focused our validation efforts on MARS2 as a proof-of-concept target because of its direct relevance to mitochondrial function. The remaining DEGs serve as a resource for hypothesis generation in future studies. Immunofluorescence and Western blot analyses demonstrated that BPA-induced suppression of MARS2 was effectively prevented by Fx treatment (Figure 4a, b). Notably, Fx significantly attenuated the upregulation of the pro-apoptotic and DNA damage marker p53 and the inflammatory signal transducer STAT1, while restoring the expression of the AR, which is essential for maintaining testicular function (Figure 4b).

Effects of Fx on the NF-κB signaling pathway in mice with testicular injury

KEGG pathway analysis implicated the NF-κB signaling pathway in the anti-inflammatory activity of Fx. The mRNA expression levels of key NF-κB pathway genes, including *Tlr4*, *Nfκb1*, *Nfκb2*, *Rela*, and *Relb*, were evaluated by reverse transcription-quantitative polymerase chain reaction (RT-qPCR). As shown in Figure 5a, BPA exposure significantly upregulated the expression of these genes compared with the control group. Protein expression of TLR4 and phosphorylation levels of IκB-α and p65—key events in NF-κB activation—were subsequently assessed by Western blotting (Figure 5b). BPA exposure markedly increased TLR4 protein levels,

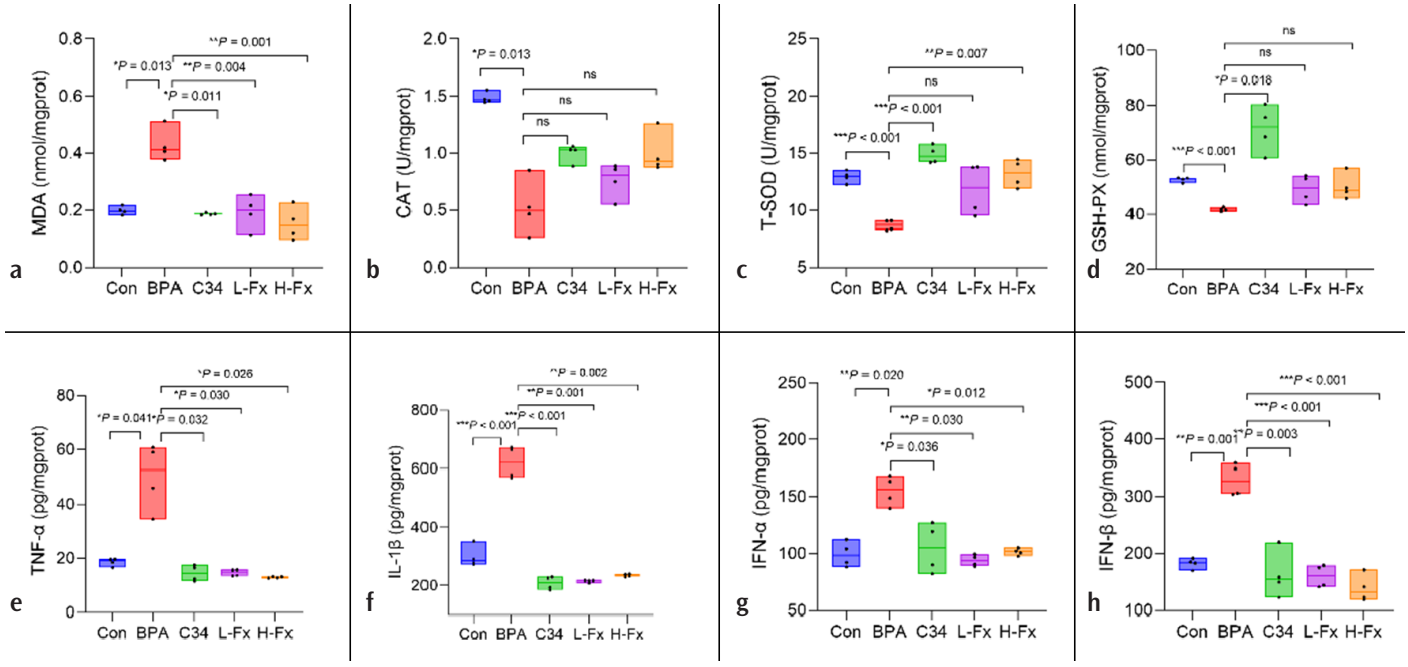

FIG. 2. Effects of Fx on oxidative stress markers and inflammatory cytokines in BPA-exposed mice. (a-d) Serum levels of MDA, CAT, T-SOD, and GSH-PX; (e-h) testicular levels of testicular TNF-α, IL-1β, IFN-α, and IFN-β. Data presentation and statistical analysis are as described for Figure 1 (n = 4). $*p < 0.05$, $**p < 0.01$, $***p < 0.001$. BPA, bisphenol A; Fx, fucoxanthin; MDA, malondialdehyde; GSH-PX, glutathione peroxidase; CAT, catalase; T-SOD, total superoxide dismutase; TNF-α, tumor necrosis factor-α; IL-1β, interleukin-1β; IFN-α, interferon-α; IFN-β, interferon-β.

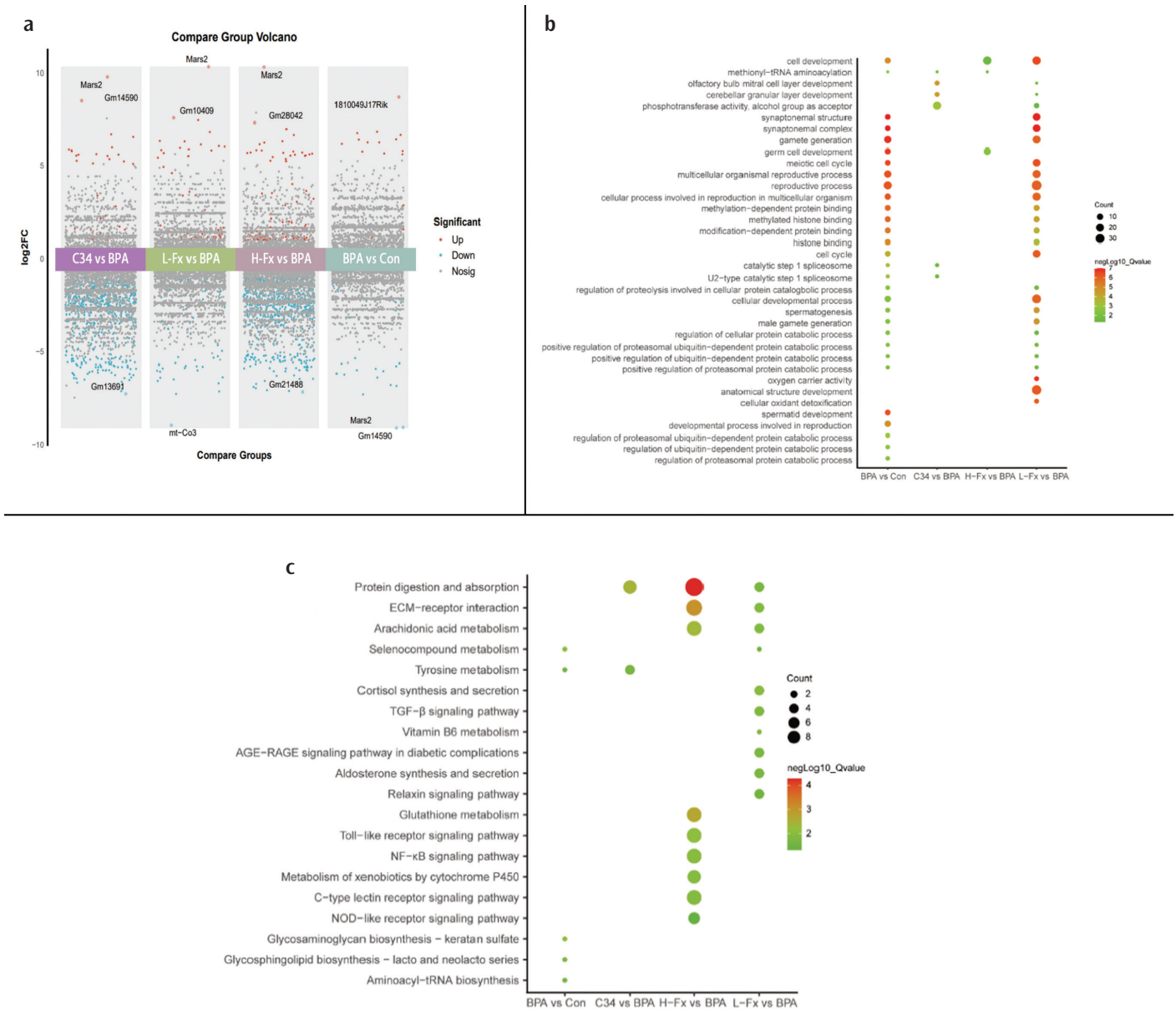

FIG. 3. Testicular transcriptome characteristics in each group. (a) Volcano plot; (b) GO enrichment analysis; (c) KEGG enrichment analysis. BPA, bisphenol A; Fx, fucoxanthin; KEGG, Kyoto Encyclopedia of Genes and Genomes; GO, Gene Ontology.

p-p65 expression, and the ratio of phospho-IκBα to total IκBα (p-IκBα/IκBα). These elevations were significantly attenuated by Fx treatment. Furthermore, immunohistochemical analysis revealed enhanced nuclear translocation of the p65 subunit in the BPA group, indicating activation of NF-κB. Although Fx treatment did not significantly alter total p65 protein expression (Figure 5c), it effectively suppressed p65 nuclear translocation. Overall, the attenuation of BPA-induced inflammation by Fx was associated with reduced activity of the TLR4/NF-κB signaling pathway.

Effects of Fx on the NLRP3/LPS-mediated pyroptosis signaling pathway in mice

Given the established link between NLRP3 inflammasome activation and pyroptosis, key molecules involved in both canonical and non-canonical pyroptosis pathways were assessed to evaluate the testicular protective effects of Fx. BPA-induced transcriptional activation of pyroptosis-related genes was significantly attenuated by C34 and Fx, as demonstrated by RT-qPCR (Figure 6a). Considering the potential involvement of the caspase-11–dependent non-canonical pyroptosis pathway, LPS localization was examined by immunofluorescence.

Intense LPS immunoreactivity was observed in Leydig cells and seminiferous tubules in the BPA group. In contrast, Fx treatment markedly reduced LPS accumulation within the seminiferous tubules (Figure 6b). Subsequent immunohistochemical (Figure 6b) and Western blot (Figure 6c) analyses further demonstrated that Fx treatment reduced the levels of key pyroptotic effectors, including NLRP3 inflammasome components, active caspases, and the cleaved form of GSDMD. In contrast, the positive control C34 did not produce a significant reduction in these specific markers under the experimental conditions.

Effects of Fx on BPA-induced inhibition of TM3 cell proliferation

To evaluate the protective effects of Fx against BPA-induced cytotoxicity in testicular interstitial cells, TM3 cells were treated with Fx either prior to or concurrently with BPA exposure. Initial cytotoxicity screening confirmed that the DMSO vehicle control did not significantly affect cell viability compared with the untreated control, validating its suitability as a solvent. Treatment with 50 μM BPA alone markedly reduced cell viability relative to the DMSO control (Figure 7a). Assessment of Fx alone revealed a concentration-dependent response: lower concentrations had no adverse effects on cell viability, whereas 50 μM Fx induced significant cytotoxicity (Figure 7b). Accordingly, subsequent experiments used 50 μM BPA, while Fx was tested at 1, 2, 5, 10, and 20 μM to determine its optimal protective concentration. As shown in Figure 7c, treatment with 5 μM Fx significantly attenuated BPA-induced cytotoxicity, restoring TM3 cell viability toward control levels. A similar protective effect was observed with 10 μM C34.

Fx alleviates BPA-induced activation of the NF-κB signaling pathway in TM3 cells

To explore the protective mechanisms of Fx against BPA-induced testicular damage, the involvement of the NF-κB pathway was investigated. Quantitative RT-PCR analysis demonstrated that

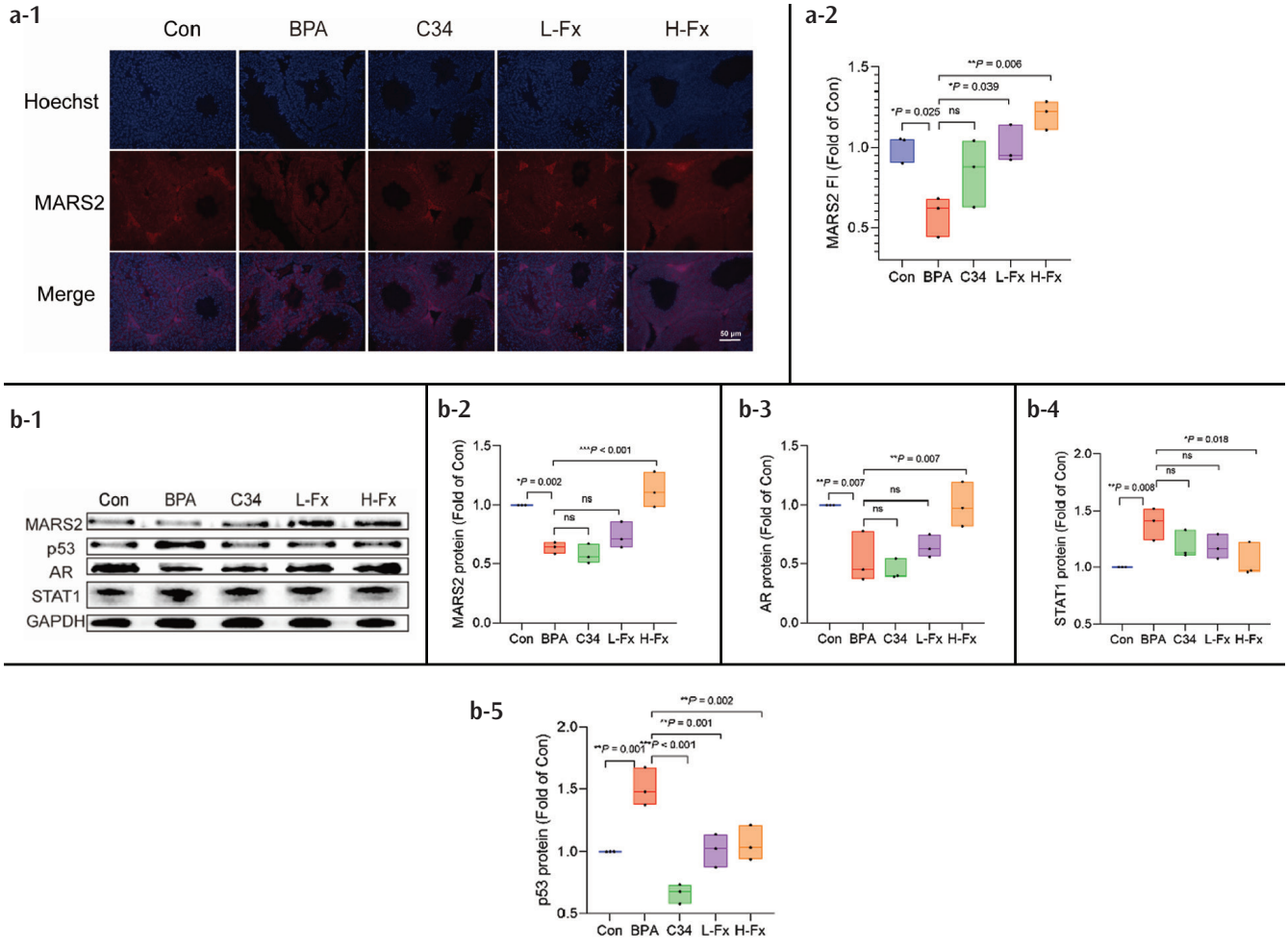

FIG. 4. Effect of Fx on oxidative stress in the mouse testis. (a) Representative immunofluorescence staining images in testicular sections for MARS2 (red) and Hoechst 33342-stained nuclei (blue) (400 ×) and its quantitative diagram; (b) the protein expression of MARS2, p53, AR, and STAT1 in mouse testis by immunoblotting assay. Data presentation and statistical analysis are as described for Figure 1 (n = 3). *$p < 0.05$, **$p < 0.01$, ***$p < 0.001$. BPA, bisphenol A; Fx, fucoxanthin; AR, androgen receptor.

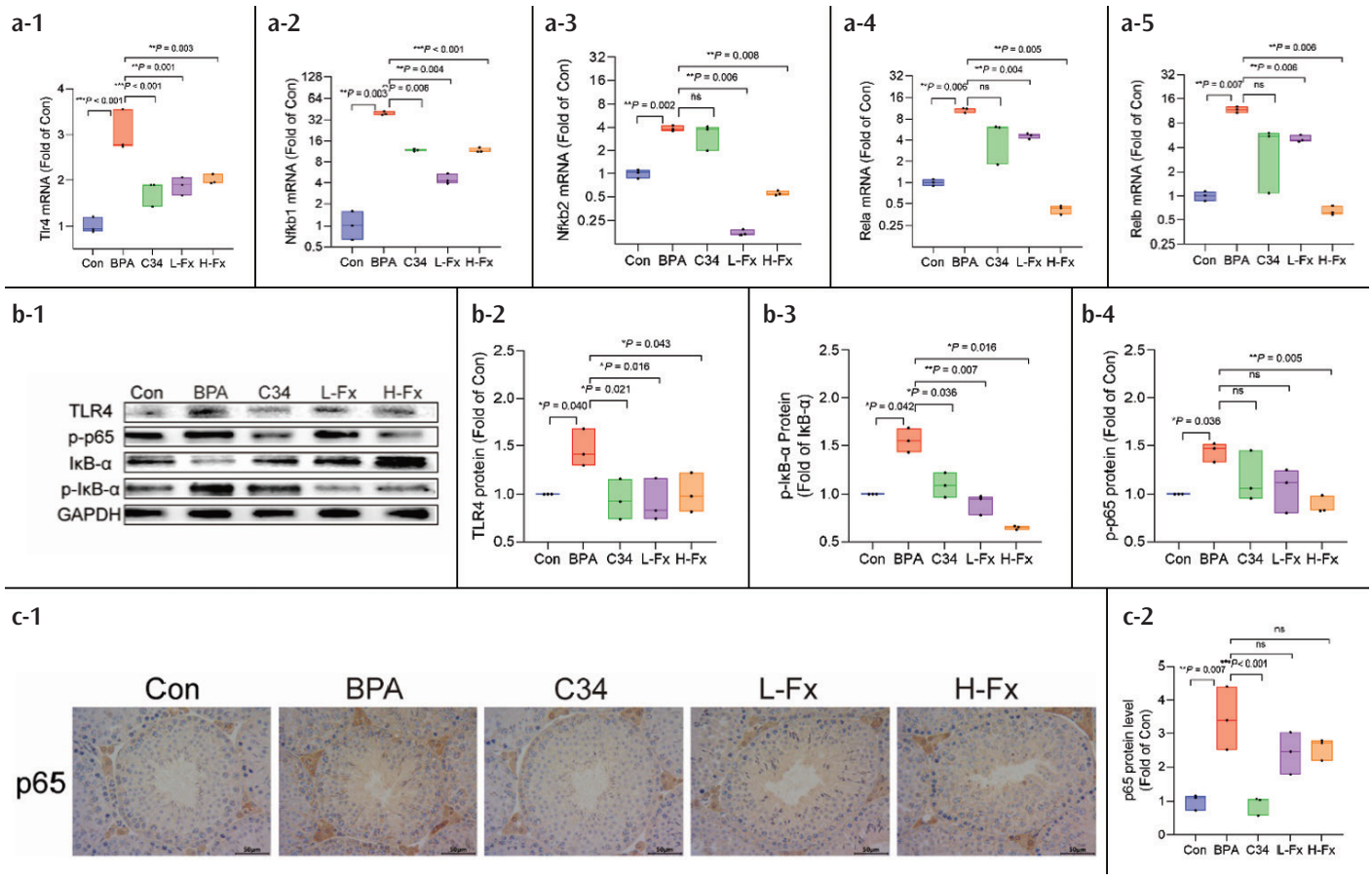

FIG. 5. Effects of Fx on NF-κB signaling pathway *in vivo*. (a) RT-qPCR analysis of mRNA levels for *Tlr4*, *Nfkb1*, *Nfkb2*, *Rela*, and *Relb*; (b) the expression of TLR4, p-p65, and p-IκBα/IκBα protein levels in mice testis by immunoblotting assay and their quantitative diagrams; (c) immunohistochemistry images showcasing p-65 protein expression (400 ×) and its quantitative diagram. Data presentation and statistical analysis are as described for Figure 1 (n = 3). *$p < 0.05$, **$p < 0.01$, ***$p < 0.001$. BPA, bisphenol A; Fx, fucoxanthin; NF-κB, nuclear factor kappa B; RT-qPCR, reverse transcription-quantitative polymerase chain reaction; p-IκBα/IκBα, phospho-IκBα to total IκBα.

BPA exposure significantly upregulated the mRNA expression of *Tlr4*, *Nlrp3*, *Rela*, *Nfkb1*, and *Nfkb2* in TM3 cells relative to controls (Figure 8a). Treatment with Fx or the positive control C34 attenuated the BPA-induced upregulation of *Tlr4*, *Nlrp3*, and *Nfkb1*. Immunofluorescence staining for NF-κB p65 indicated that BPA markedly induced nuclear translocation of p65, a hallmark of pathway activation (Figure 8b). Co-treatment with Fx or C34 suppressed this effect, maintaining p65 localization in the cytoplasm and reducing its overall signal intensity.

Fx alleviates BPA-induced pyroptosis in TM3 cells

To determine whether Fx mitigates BPA-induced pyroptosis, the expression of pyroptosis-related markers was examined in TM3 cells. BPA exposure triggered a pyroptotic response, evidenced by transcriptional upregulation of *Casp1* and *Gsdmd* (Figure 9a, b), increased proteolytic cleavage of Caspase-1 and GSDMD (Figure 9c-f) and elevated secretion of the mature cytokines IL-18 and IL-1β into the culture supernatant (Figure 9g, h). Fx treatment attenuated BPA-induced mRNA expression of *Casp1* and *Gsdmd*. At the protein level, Fx reduced proteolytic activation of Caspase-1 and GSDMD, resulting in a significant decrease in IL-18 and IL-1β secretion. Notably, the positive control C34 did not significantly suppress Caspase-1 cleavage under the experimental conditions (Figure 9d).

DISCUSSION

Carotenoids are well-recognized natural compounds with potent antioxidant properties, providing protection against diverse toxic insults, including environmental pollutant–induced testicular damage.[30-33] In this study, we employed an integrated approach to investigate the protective mechanisms of the marine carotenoid Fx against BPA-induced testicular injury. Collectively, our findings support a model in which Fx mitigates BPA-induced testicular injury by simultaneously targeting multiple nodes within a pathogenic cascade involving oxidative stress, NF-κB–driven inflammation, NLRP3 inflammasome activation, and pyroptotic cell death.

BPA is known to disrupt the antioxidant defense system in the testes.[34,35] Consistent with this, our study demonstrated that Fx alleviates BPA-induced oxidative stress, providing a foundational

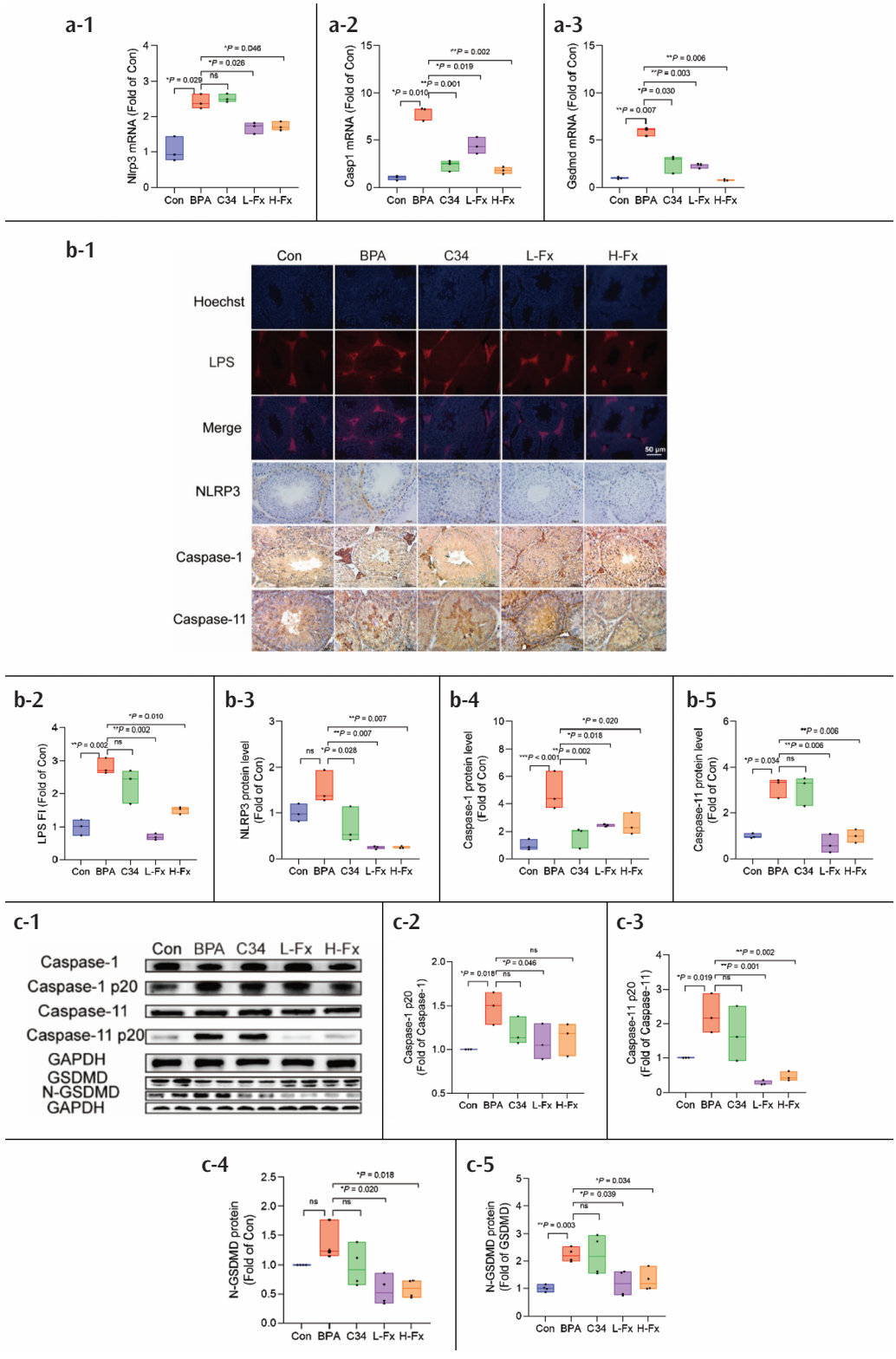

FIG. 6. Effects of Fx on the pyroptosis signaling pathway *in vivo*. (a) RT-qPCR analysis of mRNA levels for *Nlrp3*, *Casp1*, and *Gsdmd*; (b) representative immunofluorescence staining images in testicular sections for LPS (red) and Hoechst 33342-stained nuclei (blue) (400 ×), immunohistochemistry images showcasing NLRP3, Caspase-1, and Caspase-11 protein expression (400 ×) and their quantitative diagrams; (c) the expression of Caspase-1 p20/Caspase-1, Caspase-11 p20/Caspase-11, N-GSDMD and N-GSDMD/GSDMD protein levels in mice testis by immunoblotting assay and their quantitative diagrams. Data presentation and statistical analysis are as described for Figure 1 (n = 3). $*p < 0.05$, $**p < 0.01$, $***p < 0.001$. BPA, bisphenol A; Fx, fucoxanthin; RT-qPCR, reverse transcription-quantitative polymerase chain reaction; LPS, lipopolysaccharide; NLRP3, nucleotide-binding oligomerization domain-like receptor family pyrin domain-containing 3; GSDMD, gasdermin D.

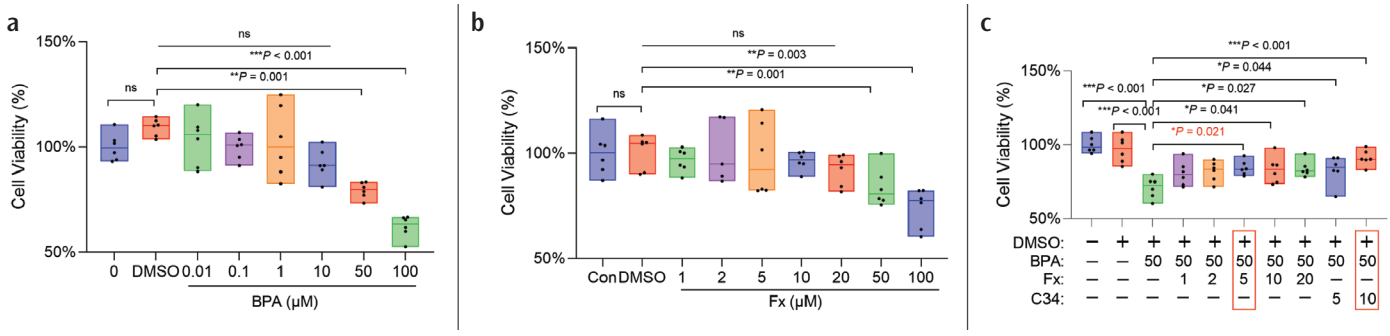

FIG. 7. Effects of Fx on TM3 cell viability in response to BPA exposure. (a) CCK-8 assay of TM3 cells treated with increasing concentrations of BPA; (b) effects of Fx alone on TM3 cell viability; (c) Fx and C34 attenuate BPA (50 μM)-induced cytotoxicity in TM3 cells. Data presentation and statistical analysis are as described for Figure 1 (n = 6). *$p < 0.05$, **$p < 0.01$, ***$p < 0.001$. BPA, bisphenol A; Fx, fucoxanthin; DMSO, dimethyl sulfoxide.

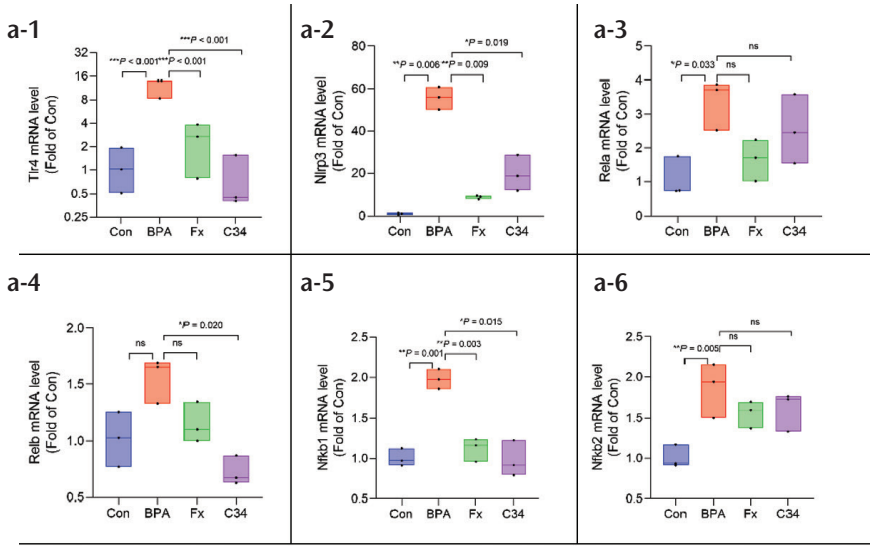

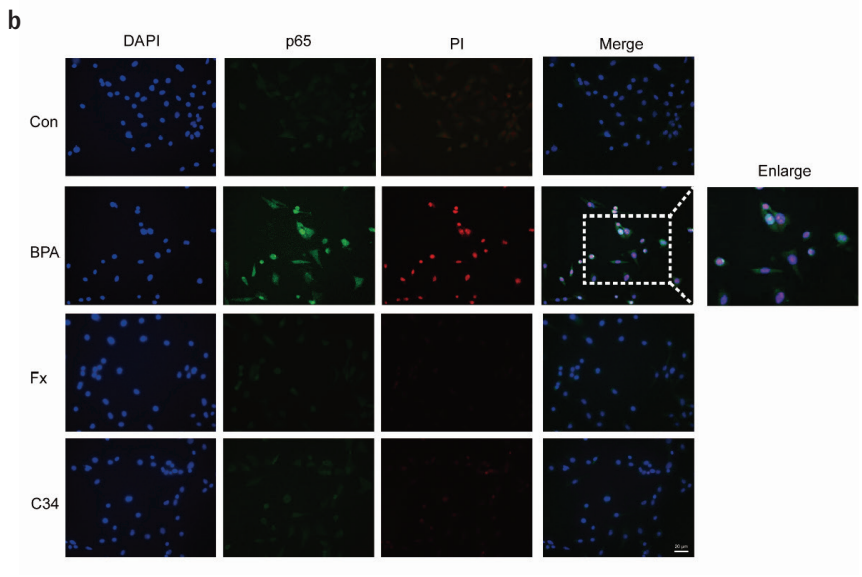

FIG. 8. Effects of Fx on NF-κB signaling pathway *in vitro*. (a) RT-qPCR analysis of mRNA levels for *Rela*, *Relb*, *Nfkb1*, *Nfkb2*, *Tlr4*, and *Nlrp3*; (b) representative immunofluorescence images in cells for p65 (green), PI (red), and DAPI-stained nuclei (blue) (400 ×). Data presentation and statistical analysis are as described for Figure 1 (n = 3). *$p < 0.05$, **$p < 0.01$, ***$p < 0.001$. BPA, bisphenol A; Fx, fucoxanthin; RT-qPCR, reverse transcription-quantitative polymerase chain reaction; NF-κB, nuclear factor kappa B.

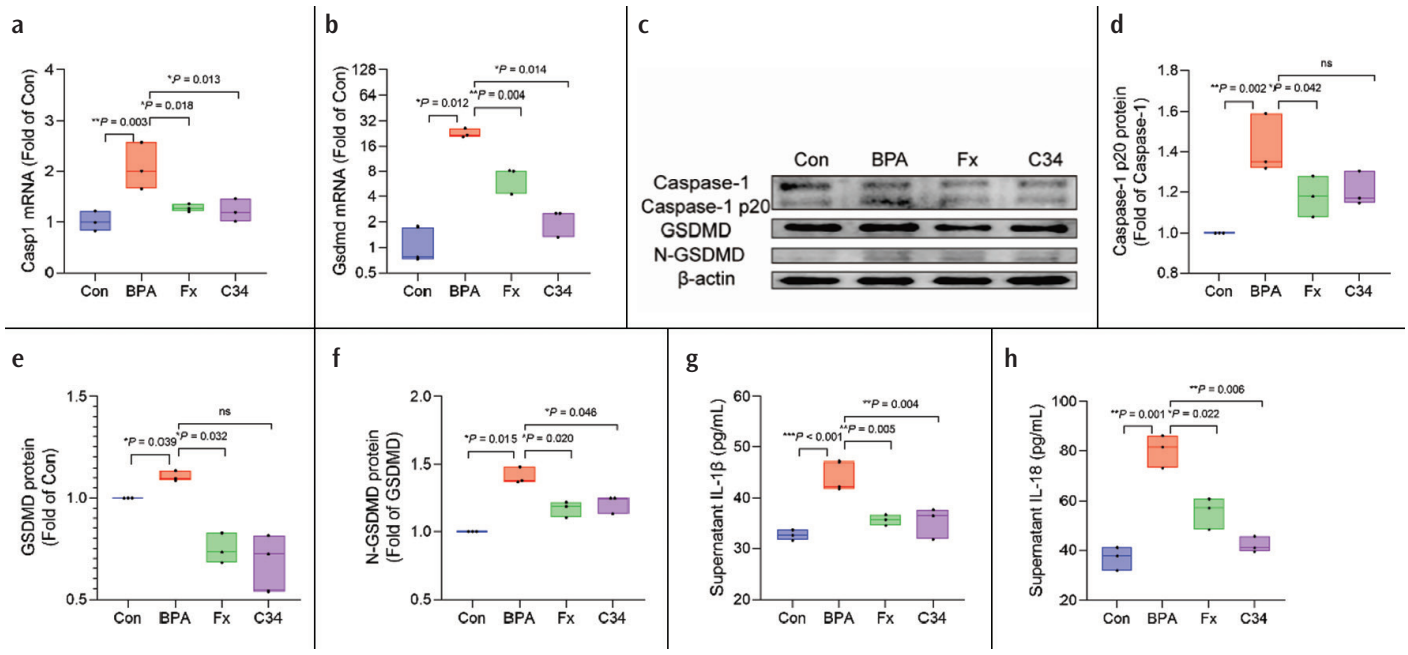

FIG. 9. Effects of Fx on the pyroptosis signaling pathway *in vitro*. (a, b) The mRNA levels of *Casp1* and *Gsdmd*; (c) Western blotting analysis of the expression of Caspase-1, Caspase-1 p20, GSDMD, and N-GSDMD; (d-f) the quantification of the Western blotting analysis; (g, h) IL-1β and IL-18 concentrations in TM3 cell supernatant. Data presentation and statistical analysis are as described for Figure 1 (n = 3). $*p < 0.05$, $**p < 0.01$, $***p < 0.001$. BPA, bisphenol A; Fx, fucoxanthin; GSDMD, gasdermin D; IL-1β, interleukin-1β; IL-18, interleukin-18.

step for its subsequent anti-inflammatory effects. To unbiasedly identify downstream events, transcriptome sequencing revealed that Fx's protective influence was closely associated with modulation of the NF-κB, NLR, and TLR signaling pathways, which are recognized as bridges linking oxidative stress to sterile inflammation.[36-38] Notably, one of the most significantly altered genes was *MARS2*, although its functional role in testicular physiology remains largely unexplored.[39,40] This finding identifies *MARS2* as a novel transcriptional target, warranting further functional investigation.

Based on these transcriptomic insights, we propose a model for BPA-induced injury in which oxidative stress activates TLR4 and subsequently NF-κB signaling. Fx treatment mitigated multiple nodes of this cascade, including reduced TLR4 expression, inhibition of p65 nuclear translocation, and downregulation of NF-κB target genes. These events likely contribute collectively to the suppression of NLRP3 inflammasome priming. Our data further link Fx's protective effects to broad inhibition of pyroptosis, as evidenced by coordinated reductions in Caspase-1/GSDMD cleavage and IL-1β/IL-18 secretion. The central role of the TLR4/NF-κB axis was supported by the positive control, the TLR4 inhibitor C34, which similarly attenuated testicular damage and inflammatory signaling. While both Fx and C34 converge on this pathway, Fx uniquely modulated *MARS2* expression *MARS2*, suggesting that its protective effects extend beyond TLR4 inhibition alone.

While streptozotocin and cisplatin are commonly used to model testicular toxicity, the BPA model employed here is particularly relevant for simulating low-dose, chronic environmental exposure. Unlike chemotherapeutic or diabetic models, BPA-induced injury may more closely reflect real-world exposure to endocrine-disrupting chemicals, highlighting the translational relevance of our findings. This study has several limitations, which also provide avenues for future research. First, the proposed TLR4–pyroptosis axis requires causal validation using genetic knockout or knockdown models. Second, the functional role of *MARS2* warrants further investigation. Third, although histological and biochemical markers were assessed, functional reproductive outcomes, such as sperm count and motility, were not evaluated. While the main cohort was adequately powered to detect large effects in primary phenotypes, the sample sizes for detailed mechanistic analyses (n = 3–6 per group) were smaller due to tissue constraints and the exploratory nature of these assays. Consequently, these analyses have limited power to detect subtle effects, and non-significant findings should be interpreted with caution. Future studies with larger sample sizes are needed to confirm these mechanistic observations and to explore effects of smaller magnitude. Moreover, although our study integrated findings from testicular tissue and a key Leydig cell model *in vitro*, future work using single-cell RNA sequencing will be crucial to dissect the protective effects of Fx on specific testicular cell populations *in vivo*.

In conclusion, our data support a model in which Fx ameliorates BPA-induced testicular injury by attenuating mitochondrial oxidative stress and coordinately downregulating key proinflammatory events, including TLR4/NF-κB signaling, NLRP3 inflammasome activation, and pyroptosis. These findings highlight the potential

of integrating Fx-rich foods or supplements into lifestyle or clinical strategies aimed at mitigating the silent risk of male reproductive dysfunction associated with chronic, low-level chemical exposure.

Ethics Committee Approval: The experimental protocol was approved by the Ethics Committee of Zhejiang Ocean University (approval number: 2023113, date: 20.12.2023).

Informed Consent: Not applicable.

Data Sharing Statement: The data that support the findings of this study are available from the corresponding author upon reasonable request.

Authorship Contributions: Concept- K.X.; Design- H.C.; Supervision- Z.Y.; Funding- Z.Y.; Materials- T.L.; Data Collection or Processing- X.R., T.L.; Analysis and/or Interpretation- H.C.; Literature Review- F.H.; Writing- K.X., X.R.; Critical Review- Z.Y., F.H.

Conflict of Interest: The authors declare that they have no conflict of interest.

Funding: This work was supported by the Zhejiang Provincial Medical and Health Technology Plan Project under Grant No. 2024KY1776.

REFERENCES

1. Vandenberg LN, Maffini MV, Sonnenschein C, Rubin BS, Soto AM. Bisphenol-A and the great divide: a review of controversies in the field of endocrine disruption. *Endocr Rev*. 2009;30:75-95. [CrossRef]
2. Huelsmann RD, Will C, Carasek E. Determination of bisphenol A: old problem, recent creative solutions based on novel materials. *J Sep Sci*. 2021;44:1148-1173. [CrossRef]
3. Guimarães AGC, Coutinho VL, Meyer A, Lisboa PC, de Moura EG. Human exposure to bisphenol A (BPA) through medical-hospital devices: a systematic review. *Environ Toxicol Pharmacol*. 2023;97:104040. [CrossRef]
4. Bahelka I, Stupka R, Čítek J, Šprysl M. The impact of bisphenols on reproductive system and on offspring in pigs - a review 2011-2020. *Chemosphere*. 2021;263:128203. [CrossRef]
5. Ma Y, Liu H, Wu J, et al. The adverse health effects of bisphenol A and related toxicity mechanisms. *Environ Res.* 2019;176:108575. [CrossRef]
6. Rahman MS, Kwon WS, Ryu DY, et al. Functional and proteomic alterations of F1 capacitated spermatozoa of adult mice following gestational exposure to bisphenol A. *J Proteome Res*. 2018;17:524-535. [CrossRef]
7. Ryu DY, Pang WK, Adegoke EO, et al. Abnormal histone replacement following BPA exposure affects spermatogenesis and fertility sequentially. *Environ Int.* 2022;170:107617. [CrossRef]
8. Shao X, Wang Y, Wang G, et al. Mitochondria-targeted nanoformulation inhibits periodontal ligament stem cells pyroptosis to promote periodontal tissue regeneration in periodontitis. *Chemical Engineering Journal*. 2025;167364. [CrossRef]
9. S Y, K L M, Harithpriya K, et al. Disruptive multiple cell death pathways of bisphenol-A. *Toxicol Mech Methods*. 2025;35:430-443. [CrossRef]
10. Ouyang Z, Zhu W, Xie Y, et al. Green tea diet can effectively antagonize the toxicity induced by environmental-related concentrations of BPA: an implication from in vivo and in silico studies. *J Agric Food Chem*. 2024;72:20633-20645. [CrossRef]
11. Shi X, Xu T, Li X, et al. ROS mediated pyroptosis-M1 polarization crosstalk participates in inflammation of chicken liver induced by bisphenol A and selenium deficiency. *Environ Pollut.* 2023;324:121392. [CrossRef]
12. Wang C, Wang L, Huang C, et al. Involvement of NLRP3/Caspase-1/GSDMD-dependent pyroptosis in BPA-induced apoptosis of human neuroblastoma cells. *Biochem Pharmacol*. 2022;200:115042. [CrossRef]
13. Zhang X, Fan M, Luo K, et al. In vivo assessment of the effects of mono-carrier encapsulated fucoxanthin nanoparticles on type 2 diabetic C57 mice and their oxidative stress. *Antioxidants (Basel)*. 2022;11:1976. [CrossRef]
14. Wang K, Huang K, Li X, et al. Kelp nanocellulose combined with fucoxanthin achieves lipid-lowering function by reducing oxidative stress with activation of Nrf2/HO-1/NQO1 pathway. *Food Chem*. 2025;464:141588. [CrossRef]
15. Agarwal S, Singh V, Chauhan K. Antidiabetic potential of seaweed and their bioactive compounds: a review of developments in last decade. *Crit Rev Food Sci Nutr*. 2023;63:5739-5770. [CrossRef]
16. Silva A, Cassani L, Grosso C, et al. Recent advances in biological properties of brown algae-derived compounds for nutraceutical applications. *Crit Rev Food Sci Nutr*. 2024;64:1283-1311. [CrossRef]
17. Sun H, Yang S, Zhao W, et al. Fucoxanthin from marine microalgae: a promising bioactive compound for industrial production and food application. *Crit Rev Food Sci Nutr.* 2023;63:7996-8012. [CrossRef]
18. Kong ZL, Sudirman S, Hsu YC, Su CY, Kuo HP. Fucoxanthin-rich brown algae extract improves male reproductive function on streptozotocin-nicotinamide-induced diabetic rat model. *Int J Mol Sci*. 2019;20:4485. [CrossRef]
19. Wang PT, Sudirman S, Hsieh MC, Hu JY, Kong ZL. Oral supplementation of fucoxanthin-rich brown algae extract ameliorates cisplatin-induced testicular damage in hamsters. *Biomed Pharmacother*. 2020;125:109992. [CrossRef]
20. Gurmeet K, Rosnah I, Normadiah MK, Das S, Mustafa AM. Detrimental effects of bisphenol A on development and functions of the male reproductive system in experimental rats. *EXCLI J*. 2014;13:151-160. [CrossRef]
21. Salian S, Doshi T, Vanage G. Neonatal exposure of male rats to Bisphenol A impairs fertility and expression of sertoli cell junctional proteins in the testis. *Toxicology*. 2009;265:56-67. [CrossRef]
22. Ling Y, Huang X, Li A, et al. Bisphenol A exposure induces testicular oxidative damage via FTO/m6A/Nrf2 axis during postnatal development in mice. *J Appl Toxicol*. 2023;43:694-705. [CrossRef]
23. Wang Y, Wu Y, Zhang S. Impact of bisphenol-A on the spliceosome and meiosis of sperm in the testis of adolescent mice. *BMC Vet Res.* 2022;18:278. [CrossRef]
24. Liu Z, Xu B, Zheng J, et al. Fucoxanthin ameliorates high-fat diet-induced kidney injury in mice. *Br J Nutr*. 2025;134:441-450. [CrossRef]
25. Wang X, Ma J, Li W, et al. BPA exacerbates zinc deficiency-induced testicular tissue inflammation in male mice through the TNF-α/NF-κB/Caspase8 signaling Pathway. *Biol Trace Elem Res*. 2025;203:4153-4163. [CrossRef]
26. Neal MD, Jia H, Eyer B, et al. Discovery and validation of a new class of small molecule Toll-like receptor 4 (TLR4) inhibitors. *PLoS One*. 2013;8:e65779. [CrossRef]
27. Kang JY, Xu MM, Sun Y, et al. Melatonin attenuates LPS-induced pyroptosis in acute lung injury by inhibiting NLRP3-GSDMD pathway via activating Nrf2/HO-1 signaling axis. *Int Immunopharmacol*. 2022;109:108782. [CrossRef]
28. Zuo X, Sun M, Bai H, et al. The effects of 17β-trenbolone and bisphenol A on sexual behavior and social dominance via the hypothalamic-pituitary-gonadal axis in male mice. *J Environ Sci (China)*. 2025;151:54-67. [CrossRef]
29. Zhao Q, Liu Y, Wang X, et al. Cuscuta chinensis flavonoids reducing oxidative stress of the improve sperm damage in bisphenol A exposed mice offspring. *Ecotoxicol Environ Saf*. 2023;255:114831. [CrossRef]
30. Yin B, Lu M, Liu X, et al. Astaxanthin alleviates di-(2-ethylhexyl) phthalate-induced testicular injury via Cdk2-mediated inhibition of cell cycle arrest and apoptosis. *J Agric Food Chem*. 2025;73:16949-16964. [CrossRef]
31. Ziamajidi N, Khajvand-Abedini M, Daei S, Abbasalipourkabir R, Nourian A. Ameliorative effects of vitamins A, C, and E on sperm parameters, testis histopathology, and oxidative stress status in zinc oxide nanoparticle-treated rats. *Biomed Res Int*. 2023;2023:4371611. [CrossRef]
32. Bahrami N, Mehrzadi S, Goudarzi M, Mansouri E, Fatemi I. Lycopene abrogates di-(2-ethylhexyl) phthalate induced testicular injury by modulating oxidative, endocrine and inflammatory changes in mice. *Life Sci*. 2018;207:265-271. [CrossRef]
33. Zhao Y, Li MZ, Shen Y, et al. Lycopene prevents DEHP-Induced leydig cell damage with the Nrf2 antioxidant signaling pathway in mice. *J Agric Food Chem.* 2020;68:2031-2040. [CrossRef]
34. Yang W, Pan F, Zhao T, et al. Bisphenol A induces apoptosis and disrupts testosterone synthesis in TM3 cells via reactive oxygen species-mediated mitochondrial pathway and autophagic flux inhibition. *Ecotoxicol Environ Saf.* 2025;289:117691. [CrossRef]
35. Maniradhan M, Sivagurunathan N, Unnikrishnan AK, Anbiah VS, Calivarathan L. Selenium ameliorates oxidized phospholipid-mediated testicular dysfunction and epididymal sperm abnormalities following Bisphenol A exposure in adult Wistar rats. *Reprod Toxicol*. 2024;130:108751. [CrossRef]
36. Liu J, Guan Y, Yang L, et al. Ferulic acid as an anti-inflammatory agent: insights into molecular mechanisms, pharmacokinetics and applications. *Pharmaceuticals (Basel)*. 2025;18:912. [CrossRef]
37. Arab HH, Alsufyani SE, Ashour AM, et al. Targeting JAK2/STAT3, NLRP3/Caspase-1, and PK2/PKR2 pathways with arbutin ameliorates lead acetate-induced testicular injury in rats. *Pharmaceuticals (Basel).* 2024;17:909. [CrossRef]

38. El Safadi M, Hassan HM, Ali A, Al-Emam A. Petunidin attenuates vinclozolin instigated testicular toxicity in albino rats via regulating TLR4/MyD88/TRAF6 and Nrf-2/Keap-1 pathway: a pharmacodynamic and molecular simulation approach. *Int Immunopharmacol.* 2024;143:113531. [CrossRef]
39. Lin SC, Karoly ED, Taatjes DJ. The human ΔNp53 isoform triggers metabolic and gene expression changes that activate mTOR and alter mitochondrial function. *Aging Cell.* 2013;12:863-872. [CrossRef]
40. Son J, Jung O, Kim JH, et al. MARS2 drives metabolic switch of non-small-cell lung cancer cells via interaction with MCU. *Redox Biol.* 2023;60:102628. [CrossRef]